Journal of Computational and Applied Mathematics 451 (2024) 116082

Contents lists available at ScienceDirect

Journal of Computational and Applied Mathematics

journal homepage: www.elsevier.com/locate/cam

A high order numerical scheme for a nonlinear nonlocal reaction–diffusion model arising in population theory

Ezio Venturino [d,1], Sebastian Aniţa [b,c], Domenico Mezzanotte [d,1], Donatella Occorsio [a,e,1,*]

[a] Department of Mathematics, Computer Science and Economics, University of Basilicata, Via dell'Ateneo Lucano 10, 85100 Potenza, Italy
[b] Faculty of Mathematics, "Alexandru Ioan Cuza" University of Iaşi, Bd. Carol I 11, Iaşi 700506, Romania
[c] "Octav Mayer" Institute of Mathematics of the Romanian Academy, Bd. Carol I 8, Iaşi 700505, Romania
[d] Department of Mathematics "Giuseppe Peano", University of Turin, Via Carlo Alberto 10, 10123 Turin, Italy
[e] C.N.R. National Research Council of Italy, IAC Institute for Applied Computing "Mauro Picone", Via P. Castellino, 111, 80131 Napoli, Italy

ARTICLE INFO

MSC:
35K57
65M20
41A10
65D32

Keywords:
Reaction diffusion equations
Line method
Generalized Bernstein polynomials

ABSTRACT

This paper provides a numerical method for nonlinear equation arising in mathematical biology. It is an extension of another one recently proposed for the linear, less realistic, situation. The main novel result is the proof that the convergence of the numerical method is of order four, as to our knowledge no similar high accuracy results exist yet in the current literature for usually employed simulation schemes for nonlocal equations.

1. Introduction

Several problems in engineering, applied mathematics and mathematical ecology require the study of situations in which the results of certain actions or situations are felt at a distance. Here we focus in particular on population theory, aiming at an extension of a previous investigation by considering a more realistic model. In [1] indeed, the population demographics is regulated by a simple balance between births and deaths, with no other vital mechanisms entering in the model. More refined models in general include the fact that even in a population of alike individuals, there is usually competition for scarce resources. In the former case, basically, the model is formulated as a Malthus equation [2]. This is unrealistic in that it leads to exponential growth in the presence of finite resources, or alternatively to exponential population extinction. The latter instead consists in introducing a correction term, first used by Verhulst, leading to what is usually known the logistic equation [3–5]. With a population growth rate that depends on the population itself, and is negatively correlated with it, the population settles to a value known as the environment carrying capacity.

The aim of this paper is thus the setting up and analysis of a numerical method of suitable high order for the logistic diffusion equation. While we retain the nonlocal effect already considered in [1], namely affecting only the population birth rate, we stress that this paper provides a nontrivial extension to a nonlinear spatial model of the numerical scheme.

* Corresponding author at: Department of Mathematics, Computer Science and Economics, University of Basilicata, Via dell'Ateneo Lucano 10, 85100 Potenza, Italy.

E-mail addresses: ezio.venturino@unito.it (E. Venturino), sanita@uaic.ro (S. Aniţa), domenico.mezzanotte@unito.it (D. Mezzanotte), donatella.occorsio@unibas.it (D. Occorsio).

[1] Member of the INdAM research group GNCS and of the group RITA.

https://doi.org/10.1016/j.cam.2024.116082
Received 12 January 2024; Received in revised form 23 March 2024
Available online 21 June 2024

Reaction–diffusion equations constitute a major field of research, in particular they have become relevant in recent years because, due to the globalization phenomenon, we are experiencing alien species invasions, with deleterious effects on the native ecosystems. For instance, species formerly unknown in temperate climates are carried in them from tropical areas and find good environmental conditions for settling. At the same time, they slowly remove the indigenous populations due to various demographic and epidemic factors [6]. Examples of this phenomenon are the establishment of the grey squirrels in the UK and Italy in the previous century [7,8]. It is to be noted that spatially the invasion mechanism is generally not uniform and leads to spatial heterogeneities [9–12]. Other instances in Italy concern the Mountain hare, which has been replaced by the European hare mainly because of imports for hunting purposes, [13], and the cottontail, which has altered the natural predator–prey interactions between the foxes and the hares, with a considerable damage for the latter, through what is known as apparent competition, [14,15]. In situations such as these, it is important to study travelling waves [16,17] and to assess the alien species invasion speed, [18]. Models closer to the one considered here also could include delays [19] as well as integro-differential terms, [20,21].

The origin of the study of nonlocal equations dates back to engineering applications. For instance, the Cahn–Hillier equation [22–24], material science [25], modified phase fields [26], for which numerically a multigrid method has been analysed [27], the Allen–Cahn equation [28] and the heat equation [29].

The paper is organized as follows. In the next section we provide some basic information for setting up the discretization of the nonlocal operator. Section 1.1 introduces the nonlinear equation for which the numerical scheme is set up. This is followed by a section devoted to an analytic investigation on the boundedness of its solution. Section 4 presents the numerical scheme in detail proving its convergence and assessing its order. A final section on numerical results supports the theoretical findings.

1.1. The model

We now briefly illustrate the problem that we want to tackle in the paper. We will consider a nonlocal version of the logistic equation for a population $u(x,t)$ subject to the following initial

$$u(x,0) = k(x) \geq 0, \quad k \in C^0([-a,a]), \tag{1}$$

and Dirichlet boundary conditions

$$u(-a,t) = b_-(t) \geq 0, \quad u(a,t) = b_+(t) \geq 0, \quad t > 0, \quad b_\pm \in C([0,\infty)), \tag{2}$$

where $k(x)$ and $b_\pm(t)$ are known functions. Further, we assume that the population reproduction rate $r \geq 0$ is constant. The nonlocal operator is defined as follows

$$\mathcal{K}(u,x,t) = \int_{-a}^{a} \varphi(y-x)u(y,t)\,dy, \tag{3}$$

where the function $\varphi(y-x)$ is sufficiently smooth. The nonlinear model with reproduction depending from distant resources reads:

$$\frac{\partial u(t)}{\partial t} = \frac{\partial^2 u(x,t)}{\partial x^2} + r\,\mathcal{K}(u,x,t) - u^2(x,t). \tag{4}$$

The quadratic term represents intraspecific competition, which occurs as mentioned above, only in the actual position occupied by the relevant individuals. For simplicity and without loss of generality, we rescale the competition coefficient to the value 1.

2. Preliminaries

Throughout the paper, C will denote a generic positive constant having different meanings at different occurrences, and by writing $C \neq C(a,b,\dots)$ we will understand that C is independent of $a,b,\dots$; $\mathbb{P}_m$ is the space of the algebraic polynomials of degree at most m. For a given function $k(x,y)$ defined in $[-a,a]\times[-a,a]$, with k_x (or k_y) we will mean that x (or y) is fixed and the function has to be considered dependent only on y (or x).

2.1. Functional spaces

For any fixed $a > 0$, let $C^0([-a,a])$ be the space of continuous functions on $[-a,a]$, equipped with the norm

$$\|f\|_\infty = \sup_{x\in[-a,a]} |f(x)|.$$

For a given function $g(x,y)$ defined in $[a_1,b_1]\times[a_2,b_2]$, the space $C^{0,0}([a_1,b_1]\times[a_2,b_2])$ denotes the space of the continuous functions w.r.t. each variable, equipped with the norm

$$\|g\|_\infty = \sup_{(x,y)\in[a_1,b_1]\times[a_2,b_2]} |g(x,y)|.$$

Furthermore, for any pair of positive integers p,q, we denote by $C^{p,q}([a_1,b_1]\times[a_2,b_2])$ the space of continuously differentiable functions $g(x,y)$ of order p w.r.t. the first variable, and of order q w.r.t. the second one.

In $C^0([-a,a])$, setting $\phi(x) := \sqrt{a^2-x^2}$, we recall the ϕ-modulus of smoothness by Ditzian and Totik [30]

$$\omega_\phi^k(f,t) = \sup_{0<h\leq t} \|\Delta_{h\phi}^k f\|, \qquad k \in \mathbb{N},$$

where

$$\Delta^k_{h\phi(x)} f(x) = \sum_{i=0}^{k} (-1)^i \binom{k}{i} f\left(x + (k-2i)\frac{h}{2}\phi(x)\right).$$

Let us also introduce the Hölder–Zygmund space of order $\lambda > 0$

$$Z_\lambda = \left\{ f \in C^0([-a,a]) : \quad \sup_{t>0} \frac{\omega^k_\phi(f,t)}{t^\lambda} < \infty, \quad k > \lambda \right\}, \tag{5}$$

equipped with the norm

$$\|f\|_{Z_\lambda} := \|f\|_\infty + \sup_{t>0} \frac{\omega^k_\phi(f,t)}{t^\lambda}, \qquad k > \lambda.$$

In the case $s \in \mathbb{N}^*$, let W_s the Sobolev space

$$W_s = \left\{ f \in C^0([-a,a]) : f^{(s-1)} \in \mathcal{AC}, \|f^{(s)}\phi^s\|_\infty < \infty \right\},$$

where $\mathcal{AC}$ denotes the space of the absolutely continuous functions on $[-a,a]$, equipped with the norm

$$\|f\|_{W_s} = \|f\|_\infty + \|f^{(s)}\phi^s\|_\infty.$$

We mention that for $s < \lambda < s+1$, $W_{s+1} \subset Z_\lambda \subset W_s$ and $\|f\|_{Z_\lambda} \le C\|f\|_{W_s}$. Finally, we recall the following inequality

$$\omega^k_\phi(f,t) \le C t^\lambda \|f\|_{Z_\lambda}, \quad \forall f \in Z_\lambda, \quad k > \lambda, \quad t > 0, \quad C \ne C(f). \tag{6}$$

2.2. Generalized Bernstein polynomials

First, we recall the definition of the Generalized Bernstein polynomials on which the corresponding quadrature is based. For a given function $f \in C^0([-a,a])$ let $B_n f$ be the nth Bernstein polynomial

$$B_n f(x) := \sum_{j=0}^{n} f(x_j) p_{n,j}(x), \quad x_j := -a + jh, \quad h = \frac{2a}{n} \quad x \in [-a,a] \tag{7}$$

where

$$p_{n,j}(x) := \binom{n}{j} \left(\frac{a+x}{2a}\right)^j \left(\frac{a-x}{2a}\right)^{n-j}. \tag{8}$$

Based on the operator $B_n : C^0([-a,a]) \to C^0([-a,a])$, and fixing the integer ℓ, we recall the definition of the ℓ−th Generalized Bernstein (GB) operator $B_{n,\ell} = I - (I - B_n)^\ell$, being I the identity operator. It is explicitly defined as

$$B_{n,\ell} = \sum_{i=0}^{\ell} \binom{\ell}{i} (-1)^{i-1} B^i_n, \quad B^i_n = B^{i-1}_n B_n, \quad B^0_n = I. \tag{9}$$

For a fixed n, the sequence of polynomials $\{B^\ell_n f\}_\ell$ requires the samples of f at the $n+1$ equispaced points of $[-a,a]$, but differently from the "father" operator B_n, the additional parameter ℓ can be suitably modulated so that the convergence rate in approximating f improves as the smoothness of f increases. Indeed, this is stated in the following convergence result due to Gonska and Zhou [31], proved for the classical Bernstein polynomial $\tilde{B}_n f$ and the generalized Bernstein polynomials $\tilde{B}_{n,\ell} f$ defined in the interval $[0,1]$:

Theorem 2.1 ([31]). *Let $\ell \in \mathbb{N}$ be fixed. Then, for all $n \in \mathbb{N}$ and for any $f \in C^0([0,1])$, setting $\phi_1(x) = \sqrt{x(1-x)}$, we have*

$$\|f - \tilde{B}_{n,\ell}(f)\|_\infty \le C \left\{ \omega^{2\ell}_{\phi_1}\left(f, \frac{1}{\sqrt{n}}\right) + \frac{\|f\|_\infty}{n^\ell} \right\}, \qquad C \ne C(n,f). \tag{10}$$

Estimate (10) highlights how the choice of the parameter ℓ improves the rate of convergence for $f \in Z_\lambda$, until $\ell \le \frac{\lambda}{2}$. In any case, ℓ can be taken arbitrarily large, independently of the smoothness of f. A discussion on the choice of ℓ can be found in [32]. A survey about the main properties of GB polynomials and their applications can be found in [33].

Now, we observe that by setting $g(y) = f(2ay - a)$, $y \in [0,1]$ we have

$$B_{n,\ell}(f,x) = \tilde{B}_{n,\ell}\left(g, \frac{a+x}{2a}\right). \tag{11}$$

and hence, by Theorem 2.1 and by the same arguments used in the proof of Theorem 3.1 in [32] the following result holds:

Theorem 2.2. *Let $\ell \in \mathbb{N}$ be fixed. Then, for all $n \in \mathbb{N}$ and for any $f \in C^0([-a,a])$, we have*

$$\|f - B_{n,\ell}(f)\|_\infty \le C \left\{ \omega^{2\ell}_{\phi}\left(f, \frac{1}{\sqrt{n}}\right) + \frac{\|f\|_\infty}{n^\ell} \right\},$$

where $\phi(x) = \sqrt{a - x^2}$, and $C \ne C(n,f)$, $C = C(a,\ell)$.

2.3. The Generalized Bernstein quadrature rule

Based on the GB sequence $\{B_{n,\ell} f\}_{n\geq 1,\ell\geq 1}$, we recall the following quadrature rule [32,34,35]

$$\begin{aligned}\int_{-a}^{a} f(y)\varphi(y-x)\,dy &= \int_{-a}^{a} B_{n,\ell}(f\varphi_x, y)\,dy + \varepsilon_{n,\ell}(f\varphi_x) \\ &=: \mathcal{K}_{n,\ell}(f,x) + \varepsilon_{n,\ell}(f\varphi_x). \end{aligned} \tag{12}$$

Setting

$$\mathbf{A} := (\mathbf{A}_{i,j}), \qquad \mathbf{A}_{i,j} := p_{n,j}(x_i), \quad i,j \in \{0,1,\dots,n\},$$
$$p_{n,i}(x) := \binom{n}{i}\left(\frac{a+x}{2a}\right)^{i}\left(\frac{a-x}{2a}\right)^{n-i}, \qquad i = 0,1,\dots,n,$$

and letting by $\mathbf{I}$ the identity matrix, for $(i,j) \in \{0,1,\dots,n\} \times \{0,1,\dots,n\}$, we denote by $c_{i,j}^{(n,\ell)}$ the entries of the matrix $C_{n,\ell}$

$$C_{n,\ell} = \mathbf{I} + (\mathbf{I}-\mathbf{A}) + \cdots + (\mathbf{I}-\mathbf{A})^{\ell-1}, \quad C_{n,1} = \mathbf{I}, \quad C_{n,\ell} \in \mathbb{R}^{(n+1)\times(n+1)}. \tag{13}$$

Then the quadrature rule $\mathcal{K}_{n,\ell}(f)$ (shortly denoted by *GB* rule) has the following expression

$$\mathcal{K}_{n,\ell}(f,x) = \sum_{j=0}^{n} f(x_j)\varphi(x_j - x) D_j^{(\ell)}, \quad D_j^{(\ell)} = \frac{2a}{n+1}\sum_{i=0}^{n} c_{i,j}^{(n,\ell)}. \tag{14}$$

Denoting by $\|B\|_\infty = \max_{0\leq k\leq n}\sum_{h=0}^{n}|B(k,h)|$ the infinity norm of a matrix $B \in \mathbb{R}^{(n+1)\times(n+1)}$ and taking into account $\|\mathbf{A}\|_\infty = 1$, we have

$$\|C_{n,\ell}\|_\infty \leq 2^{\ell} - 1, \tag{15}$$

and hence

$$\sup_n \sum_{j=0}^{n} |D_j^{(\ell)}| < \infty,$$

i.e., fixing ℓ, the GB rule is stable in $C^0([-a,a])$. Now, about the quadrature error

$$\varepsilon_{n,\ell}(f\varphi_x) := \int_{-a}^{a} [f(y)\varphi_x(y) - B_{n,\ell}(f\varphi_x, y)]\,dy, \tag{16}$$

we can prove the following result

Theorem 2.3. *Under the assumption*

$$\mathcal{N}_\lambda := \sup_{x\in[-a,a]} \|f\varphi_x\|_{Z_\lambda}, \quad 0 < \lambda < 2\ell,$$

we have

$$\sup_{x\in[-a,a]} |\varepsilon_{n,\ell}(f\varphi_x)| \leq C\left\{\frac{\mathcal{N}_\lambda}{(\sqrt{n})^\lambda} + \frac{\|f\|_\infty}{n^\ell}\right\}, \quad C \neq C(n,f,\varphi),\ C = C(a,\ell). \tag{17}$$

Proof. By Theorem 2.2, we get

$$|\varepsilon_{n,\ell}(f\varphi_x)| \leq 2a\|f - B_{n,\ell} f\|_\infty \leq C\left\{\omega_\varphi^{2\ell}\left(f, \frac{1}{\sqrt{n}}\right) + \frac{\|f\|_\infty}{n^\ell}\right\}$$

and by (6) it follows

$$|\varepsilon_{n,\ell}(f\varphi_x)| \leq 2a\left(\frac{\mathcal{N}_\lambda}{\sqrt{n^\lambda}} + \frac{\|f\|_\infty}{n^\ell}\right)$$

Taking the supremum on $x \in [-a,a]$, (17) follows. □

Remark 2.4. Estimate (17) generalizes the one obtained in [34,35], when $f\varphi_x$ belongs to the Sobolev space W_s, $s \in \mathbb{N}, s < \lambda < s+1$.

2.4. Some computational details

The largest effort in computing the quadrature rule depends on the matrix $C_{n,\ell}$. Now we present some properties, for which a strong computational saving can be achieved. Let us start from the matrix A, which can be constructed by rows by using the recurrence relation

$$\begin{cases} p_{n,k}(x) = \dfrac{(a-x)}{2a} p_{n-1,k}(x) + \dfrac{(a+x)}{2a} p_{n-1,k-1}(x), & k = 0,1,\dots,n, \quad n \geq 1, \\ p_{n,k}(x) = 0, & k < 0 \text{ or } k > n. \end{cases} \tag{18}$$

In this way, $\mathcal{O}(n^2)$ floating point operations are needed for each row, and using the property that A is a centrosymmetric matrix, it will be enough to compute at most $\frac{n+1}{2}$ rows. Furthermore, using the property that the product of two centrosymmetric matrices of order $n+1$ is performable into $\mathcal{O}((n+1)^3/2)$ floating point operations, the matrix $C_{n,\ell}$ can be obtained in $\mathcal{O}((\ell-2)(n+1)^3/2)$ floating point operations since it requires $\ell - 2$ products of centrosymmetric matrices.

On the other hand, as Theorem 2.3 shows, the higher the additional parameter ℓ is, the better is the rate of convergence; this however occurs until a certain threshold $\bar{\ell}$ related to the smoothness of the integrand. In this sense, in all the cases for which the integrand is very smooth, it can be useful to take into account the following recurrence relation for the matrix $C_{n,\ell}$, holding for $\ell = 2^p,\ p \in \mathbb{N}$:

$$C_{n,2^p} = C_{n,2^{p-1}} + (\mathbf{I} - \mathbf{A})^{2^{p-1}} C_{n,2^{p-1}}. \tag{19}$$

3. Boundedness of the solutions of the initial–boundary value problem

Let us recall (V. Barbu, Partial Differential Equations and Boundary Value Problems, Kluwer Acad. Publ., Dordrecht, 1998, and H. Brézis, Analyse Fonctionnelle. Théorie et Applications, Dunod, Paris, 2005) that for nonhomogeneous Dirichlet boundary conditions a weak solution is defined as

$$u = u_1 + u_2,$$

where u_1 satisfies the nonhomogeneous boundary conditions and u_2 is the weak solution of a related problem with homogeneous Dirichlet boundary conditions. The definition of the weak solution u_2 in this case uses the test functions.

Assume from now on that r is a positive constant, b_- and b_+ are nonnegative functions, $b_-, b_+ \in C^1([0,+\infty))$ and $\varphi \in C^0([-2a,2a])$, $\varphi(x) \geq 0,\ \forall x \in [-2a,2a]$.

Definition 1. Let us set $\Omega = (-a,a)$. The function u is a weak solution of the linear initial–boundary value problem

$$\frac{\partial u(x,t)}{\partial t} = \frac{\partial^2 u(x,t)}{\partial x^2} + r\int_{-a}^{a} \varphi(y-x)u(y,t)\, dy + \gamma(x,t)u(x,t) + G(x,t), \quad (x,t) \in \Omega \times (0,+\infty) \tag{20}$$

together with (1) and (2), if there exists $u_1 \in C^{2,1}(\overline{\Omega} \times [0,+\infty))$ such that

$$u_1(-a,t) = b_-(t), \quad u_1(a,t) = b_+(t), \quad \forall t \in [0,+\infty)$$

and $u_2 = u - u_1$ is a weak solution of

$$\begin{aligned} \frac{\partial u_2(x,t)}{\partial t} &= \frac{\partial^2 u_2(x,t)}{\partial x^2} + r\int_{-a}^{a} \varphi(y-x)u_2(y,t)\, dy + \gamma(x,t)u_2(x,t) + F(x,t), \\ F(x,t) &= G(x,t) - \frac{\partial u_1(x,t)}{\partial t} + \frac{\partial^2 u_1(x,t)}{\partial x^2} + r\int_{-a}^{a} \varphi(y-x)u_1(y,t)\, dy + \gamma(x,t)u_1(x,t) \end{aligned} \tag{21}$$

with now homogeneous boundary conditions for every $t \in [0,+\infty)$ and the following initial condition

$$u_2(-a,t) = 0, \quad u_2(a,t) = 0, \quad t \geq 0, \quad u_2(x,0) = k(x) - u_1(x,0), \quad x \in \Omega. \tag{22}$$

Actually u_2 is the unique weak solution of the problem (21)–(22). The definition of the weak solution u_2 in this case uses the test functions (see V. Barbu, H. Brezis).

Definition 2. u is a weak solution of (4), (1) and (2) if there exists $u_1 \in C^{2,1}(\overline{\Omega} \times [0,+\infty))$ such that

$$u_1(-a,t) = b_-(t), \quad u_1(a,t) = b_+(t), \quad \forall t \in [0,+\infty)$$

and $u_2 = u - u_1$ is a weak solution of

$$\begin{aligned} \frac{\partial u_2(x,t)}{\partial t} &= \frac{\partial^2 u_2(x,t)}{\partial x^2} + r\int_{-a}^{a} \varphi(y-x)u_2(y,t)\, dy + \gamma(x,t)u_2(x,t) + F(x,t), \\ \gamma(x,t) &= -2u_1(x,t) - u_2(x,t), \\ F(x,t) &= -u_1^2(x,t) - \frac{\partial u_1(x,t)}{\partial t} + \frac{\partial^2 u_1(x,t)}{\partial x^2} + r\int_{-a}^{a} \varphi(y-x)u_1(y,t)\, dy, \end{aligned} \tag{23}$$

with now homogeneous boundary conditions for every $t \in [0,+\infty)$ and the initial condition (22).

If we take

$$u_1(x,t) = b_-(t)\frac{a-x}{2a} + b_+(t)\frac{a+x}{2a}$$

and $b_-, b_+ \in C^1([0,+\infty))$, then $u_1 \in C^{2,1}(\overline{\Omega}\times[0,+\infty))$ and satisfies the nonhomogeneous boundary conditions.

Let us show that if $u_1 + u_2$ and $\tilde{u}_1 + \tilde{u}_2$ are both nonnegative weak solutions of (4), (1) and (2), then $\tilde{u}_1 + \tilde{u}_2 = u_1 + u_2$.

Indeed, $w = u_1 + u_2 - \widetilde{u}_1 - \widetilde{u}_2$ is a weak solution of the following problem

$$\frac{\partial w(x,t)}{\partial t} = \frac{\partial^2 w(x,t)}{\partial x^2} + r\int_{-a}^{a}\varphi(y-x)w(y,t)\,dy - (u_1(x,t)+u_2(x,t)+\widetilde{u}_1(x,t)+\widetilde{u}_2(x,t))w(x,t),$$
$$(x,t)\in\Omega\times(0,+\infty)$$
$$w(-a,t)=0,\quad w(a,t)=0,\quad t\ge 0,\quad w(x,0)=0,\quad x\in\Omega,$$

which has a unique weak solution $w = 0$ (this follows in a standard manner).

Remark 3.1. The problem (20), (1), (2) with $\gamma = 0$, $G = 0$ admits a unique weak solution. This follows via Banach's fixed point theorem.

We now prove that (4), (1) and (2) admits a unique nonnegative weak solution u. Specifically, we have the following result.

Theorem 3.2. *If $b_\pm \in C^1([0,+\infty))$ are bounded functions, the nonnegative weak solution of the initial–boundary value model (4), (1), (2) with the nonlocal term (3) is bounded.*

Proof. If u is such a weak solution, then $0 \le u(x,t) \le v(x,t)$ a.e. $(x,t)\in\Omega\times(0,+\infty)$, where v is the weak solution (which is also nonnegative) of

$$\frac{\partial v(x,t)}{\partial t} = \frac{\partial^2 v(x,t)}{\partial x^2} + r\int_{-a}^{a}\varphi(y-x)v(y,t)\,dy,\quad (x,t)\in\Omega\times(0,+\infty) \tag{24}$$
$$v(-a,t)=b_-(t),\quad v(a,t)=b_+(t),\quad t\ge 0,\quad v(x,0)=k(x),\quad x\in\Omega.$$

We get that for any $T>0$, $v\in L^\infty(\Omega\times(0,T))$ by a comparison result. Using now a fixed point result on the space

$$X = \left\{\zeta\in C([0,T];L^2(\Omega)); 0\le\zeta(x,t)\le v(x,t)\quad \text{a.e.}\ \right\}$$

we get indeed that (4), (1) and (2) admits a unique nonnegative weak solution.

Assume that b_- and b_+ are bounded functions. Let $\widetilde{u}(t)$ satisfy the following logistic equation

$$\frac{d\widetilde{u}(t)}{dt} = A\widetilde{u}(t) - \widetilde{u}(t)^2,\quad \widetilde{u}(0)=\widetilde{u}_0, \tag{25}$$

where A and $\widetilde{u}_0$ are positive constants to be defined later. Eq. (25) is a Bernoulli equation with solution

$$\widetilde{u}(t) = \frac{\widetilde{u}_0 A\exp(At)}{\widetilde{u}_0\exp(At)+A-\widetilde{u}_0},\quad t\in[0,+\infty),$$

and obviously satisfies $\widetilde{u}(t)\in[\min\{\widetilde{u}_0, A\}, \max\{\widetilde{u}_0, A\}]$ for all $t\ge 0$. Let us take

$$\widetilde{u}_0 = \max\left\{\|k\|_\infty, \|b_-\|_\infty, \|b_+\|_\infty\right\}$$

and

$$A = \max\{2ra\|\varphi\|_\infty, \|b_-\|_\infty, \|b_+\|_\infty\}.$$

It follows that $\widetilde{u}$, which is space-independent, satisfies

$$\frac{\partial\widetilde{u}(x,t)}{\partial t} = \frac{\partial^2\widetilde{u}(x,t)}{\partial x^2} + r\int_{-a}^{a}\varphi(y-x)\widetilde{u}(y,t)\,dy - \widetilde{u}(x,t)^2 + A\widetilde{u}(x,t) - r\int_{-a}^{a}\varphi(y-x)\widetilde{u}(y,t)dy \tag{26}$$
$$= \frac{\partial^2\widetilde{u}(x,t)}{\partial x^2} + r\int_{-a}^{a}\varphi(y-x)\widetilde{u}(y,t)\,dy - \widetilde{u}(x,t)^2 + f^0(x,t),\quad (x,t)\in\Omega\times(0,+\infty)$$
$$\widetilde{u}(-a,t)=\widetilde{u}(t)\ge b_-(t),\quad \widetilde{u}(a,t)=\widetilde{u}(t)\ge b_+(t),\quad t\ge 0,\quad \widetilde{u}(x,0)=\widetilde{u}(0)\ge k(x),\quad x\in\Omega,$$

where

$$f^0(x,t) = A\widetilde{u}(t) - r\widetilde{u}(t)\int_{-a}^{a}\varphi(y-x)dy \ge 0,\quad \text{a.e. } (x,t)\in\Omega\times(0,+\infty).$$

Let us prove that $u(x,t)\le\widetilde{u}(t)$ a.e. $(x,t)\in\Omega\times(0,+\infty)$. Indeed, let $w=\widetilde{u}-u$; further let $b^-(t)=\widetilde{u}(t)-b_-(t)$, $b^+(t)=\widetilde{u}(t)-b_+(t)$, $t\ge 0$, $\overline{k}(x)=\widetilde{u}_0-k(x)$, $x\in\Omega$. Then w is a weak solution of

$$\frac{\partial w(x,t)}{\partial t} = \frac{\partial^2 w(x,t)}{\partial x^2} + r\int_{-a}^{a}\varphi(y-x)w(y,t)\,dy - (\widetilde{u}(t)+u(x,t))w + f^0(x,t),\quad (x,t)\in\Omega\times(0,+\infty)$$
$$w(-a,t)=b^-(t)\ge 0,\quad w(a,t)=b^+(t)\ge 0,\quad t\ge 0,\quad w(x,0)=\overline{k}(x)\ge 0,\quad x\in\Omega.$$

This implies the following inequalities:

$$-\frac{1}{2}\int_{-a}^{a}|w^-(x,t)|^2\,dx \geq \int_0^t\int_{-a}^{a}\left|\frac{\partial w^-(x,s)}{\partial x}\right|^2 dx\,ds \qquad (27)$$
$$+r\int_0^t\int_{-a}^{a}\int_{-a}^{a}\varphi(y-x)[w^+(y,s)-w^-(y,s)]dy\,w^-(x,s)dx\,ds$$
$$-\int_0^t\int_{-a}^{a}f(x,s)[w^+(x,s)-w^-(x,s)]w^-(x,s)dx\,ds$$

where $f=\widetilde{u}+u\geq 0$. Now the right hand side of (27) is further bounded below by

$$-r\|\varphi\|_\infty\int_0^t\int_{-a}^{a}\int_{-a}^{a}w^-(y,s)w^-(x,s)dy\,dx\,ds$$

and for all $t\geq 0$ this implies the inequality

$$\|w^-(t)\|_2^2\leq 4ar\|\varphi\|_\infty\int_0^t\|w^-(s)\|_2^2ds,\qquad \forall t\geq 0$$

(where $\|\cdot\|_2$ is the usual norm of $L^2(\Omega)$). By Gronwall's inequality we finally obtain $w^-(t)=0$ in $L^2(\Omega)$ for all $t\in[0,+\infty)$ and so $u(x,t)\leq\widetilde{u}(t)$ a.e. $x\in\Omega$, $\forall t\geq 0$.

Since $\widetilde{u}$ is bounded, it follows that u is bounded as well. □

Remark 3.3. If the nonnegative weak solution u to (4), (1), (2) satisfies $u=u_1+u_2$, as in the definition, with

$$u_1(-a,t)=b_-(t),\quad u_1(a,t)=b_+(t),\quad \forall t\in[0,+\infty)$$

and

$$u_1(x,0)=k(x),\quad \forall x\in\Omega,$$

then $u\in C^l(\overline{\Omega}\times[0,+\infty))$ (where l is a prescribed positive integer) if φ and u_1 are sufficiently smooth. That follows by using a boot-strap argument and Theorems X.11-X-13 in H. Brezis.

Note that there exists such a smooth u_1 if b_-,b_+,k are sufficiently smooth and if k satisfies appropriate compatibility conditions.

4. Analysis of the numerical method

We discretize (4) by means of the method of lines that we describe here below.

Let us introduce the following spatial mesh of $n+1$ equally spaced nodes:

$$x_i=-a+hi,\quad i=0,1,\dots,n,\quad h=\frac{2a}{n}.$$

The Eqs. (4) are collocated at the $n-1$ internal nodes x_i, $i=1,\dots,n-1$, while to assess the solution values at the endpoints $x_0=-a$ and $x_n=a$ the boundary conditions (2) are employed.

In so doing, the restriction of the solution at the internal nodes x_i becomes a function solely of time, i.e.

$$u_i(t)=u(x_i,t). \qquad (28)$$

On this discretized system, we will apply the Runge–Kutta–Fehlberg scheme of order (4,5). There is still the need of taking care of the second partial derivatives in space. They are discretized by means of suitable divided difference scheme of order $\mathcal{O}(h^4)$ in space, see e.g. [36], to keep the same order of accuracy as for the one in time. However, we need to distinguish between the internal nodes from those that are close to the boundary. To be more precise, at the nodes x_i, $i=2,\dots,n-2$ we make use of the five points classical central finite difference scheme. At the points x_1 and x_{n-1} finite difference formulae are employed that are subject to two constraints. They must use only nodes in the mesh and must retain the same fourth order accuracy as for the classical ones. They can be constructed by the method of undetermined coefficients, [37,38], or simply found in tables, [36].

Finally, we discretize the integrals $\mathcal{K}(u,x,t)$ by means of the quadrature formula (12) previously introduced. In this way, the discretization reads

$$\mathcal{K}_n(u,x,t)=\sum_{j=0}^{n}\varphi(x_j-x)u(x_j,t)D_j^{(\ell)}. \qquad (29)$$

Note that from (1), the discretized initial conditions become

$$u_i(0)=k(x_i),\quad i=0,\dots,n. \qquad (30)$$

At the endpoints $x_0=-a$ and $x_n=a$ the boundary conditions (2) are employed giving the remaining two equations

$$u_0(t)=b_-(t),\quad u_n(t)=b_+(t). \qquad (31)$$

We now consider (4). The spatial derivatives for the diffusion term are discretized as follows

$$\begin{aligned}
\frac{du_1(t)}{dt} &= \frac{1}{h^2}\left[\frac{5}{6}u_0(t) - \frac{15}{12}u_1(t) - \frac{1}{3}u_2(t) + \frac{7}{6}u_3(t) - \frac{1}{2}u_4(t)\right.\\
&+ \left.\frac{1}{12}u_5(t)\right] + r\,\mathcal{K}_n(u, x_1, t) - u_1^2(t),\\
\frac{du_i(t)}{dt} &= \frac{1}{h^2}\left[-\frac{1}{12}u_{i-2}(t) + \frac{4}{3}u_{i-1}(t) - \frac{5}{2}u_i(t) + \frac{4}{3}u_{i+1}(t)\right.\\
&- \left.\frac{1}{12}u_{i+2}(t)\right] + r\,\mathcal{K}_n(u, x_i, t) - u_i^2(t), \quad i = 2, \dots, n-2,\\
\frac{du_{n-1}(t)}{dt} &= \frac{1}{h^2}\left[\frac{1}{12}u_{n-5}(t) - \frac{1}{2}u_{n-4}(t) + \frac{7}{6}u_{n-3}(t) - \frac{1}{3}u_{n-2}(t)\right.\\
&- \left.\frac{15}{12}u_{n-1}(t) + \frac{5}{6}u_n(t)\right] + r\,\mathcal{K}_n(u, x_{n-1}, t) - u_{n-1}^2(t).
\end{aligned} \tag{32}$$

The restriction of the solution at the mesh points is now

$$g_i(t, u_i(t)) = D_{xx}u(x_i, t) + r\,\mathcal{K}(u, x_i, t) - u^2(x_i, t), \quad i = 1, \dots, n-1. \tag{33}$$

$$\widetilde{g}_i(t, u_i(t)) = \widetilde{D}_{xx}u(x_i, t) + r\,\mathcal{K}_n(u, x_i, t) - u^2(x_i, t), \quad i = 1, \dots, n-1. \tag{34}$$

To this system we apply the RKF method, obtaining the discretized solution $\widetilde{g}_i(\widehat{u}_i)$, $i = 1, \dots, n-1$. Let $\widehat{u}_i(t)$, $i = 1, \dots, n-1$, denote the solution obtained by the Runge–Kutta–Fehlberg (4,5) method, and set $\widehat{u}_{i,n} := \widehat{u}_i(t_n)$, $i = 1, \dots, n-1$.

We now turn to the convergence proof. Specifically we have the following result.

Theorem 4.1. *The proposed numerical scheme has a convergence order given by (39). In particular, for very smooth kernels, we achieve order $O(h^4)$.*

Proof. First of all, note that the discretization procedure gives a system of ordinary differential equations whose right hand sides are Lipschitz continuous, so that the convergence results of the Runge–Kutta method applies.

Hence we get

$$\|u_i - \widehat{u}_i\|_\infty \sim \mathcal{O}(h^4). \tag{35}$$

Recalling (33) and (34), the error is split into three contributions,

$$\|g_i(u_i) - \widetilde{g}_i(\widehat{u}_i)\|_\infty \le \|D_{xx}u_i - \widetilde{D}_{xx}\widehat{u}_i\|_\infty + |r|\,\|\mathcal{K}(u_i) - \mathcal{K}_n(\widehat{u}_i)\|_\infty + \|u_i^2 - \widehat{u}_i^{\,2}\|_\infty. \tag{36}$$

The last term can be estimated as follows:

$$\|u_i^2 - \widehat{u}_i^{\,2}\|_\infty = \|(u_i - u_i + u_i + \widehat{u}_i)(u_i - \widehat{u}_i)\|_\infty \le \|u_i - \widehat{u}_i\|_\infty^2 + 2\|u_i\|_\infty \|u_i - \widehat{u}_i\|_\infty. \tag{37}$$

Finally, using the boundedness result of Theorem 3.2 on $\|u_i\|$, we can write

$$\|u_i^2 - \widehat{u}_i^{\,2}\|_\infty \le \|u_i - \widehat{u}_i\|_\infty [\|u_i - \widehat{u}_i\|_\infty + U] \tag{38}$$

for some $U > 0$. We are now able to estimate the right-hand side of (37), i.e. of the third term in (36). Collecting all these results, namely (35), (36), (37) and (38), we obtain

$$\begin{aligned}
&\|g_i(u_i) - \widetilde{g}_i(\widehat{u}_i)\|_\infty \le \|D_{xx}u_i - \widetilde{D}_{xx}\widehat{u}_i\|_\infty + |r|\,\|\mathcal{K}(u_i) - \mathcal{K}_n(\widehat{u}_i)\|_\infty + \|u_i^2 - \widehat{u}_i^{\,2}\|_\infty\\
&\le O(h^4) + O(h^{\frac{s}{2}}) + O(h^4) = \max\left\{O(h^{\frac{s}{2}}), O(h^4)\right\}. \quad \square \quad \square
\end{aligned} \tag{39}$$

Remark 4.2. Hence we discover that the results of a similar linear problem [1] extend also to this more realistic nonlinear case.

5. Numerical examples

This section highlights the reliability of the proposed method for the nonlinear problem (4), (1), (2). We will consider various choices of kernel functions $\varphi(y - x)$, as well as different initial conditions $k(x)$ and Dirichlet boundary conditions $b_\pm(t)$. To make direct comparisons in similar contexts possible, we keep the quantities $a = 2$ and $T = 10$ fixed in all the examples.

All the tests are performed in double precision on the Matlab 2022a software installed on a MacBook Pro laptop under the macOS operating system.

Table 1
Example 5.1, problem (40) — Empirical Order of Convergence.

n	$e_n(u)$	EOC_n
8	9.14e−03	
16	1.29e−04	6.14
32	1.84e−05	2.82
64	1.10e−06	4.06
128	1.03e−07	3.42
256	3.41e−09	4.91
512	9.42e−10	1.86
	$\mathrm{EOC}_{\mathrm{mean}}$	3.87

Table 2
Example 5.2, problem (41) — Empirical Order of Convergence.

n	$e_n(u)$	EOC_n
8	1.17e−02	
16	1.76e−04	6.05
32	9.94e−05	8.24
64	2.40e−06	5.37
128	2.02e−07	3.57
256	6.46e−09	4.97
512	3.07e−10	4.40
	$\mathrm{EOC}_{\mathrm{mean}}$	4.20

5.1. Tests with known solution

We start taking into exam examples in which the analytical solution of the model is known a priori. In this context, we evaluate the maximum relative errors attained by our numerical scheme approximating the solution $u^*(x,t)$ for increasing values of n to test its accuracy. Hence, denoting by $\widehat{u}_n(x,t)$ the solution of the discretized model and by M a fixed integer, here taken to be 9, we report the error, the Empirical Order of Convergence (EOC) and the Mean Empirical Order of Convergence defined as follows

$$e_n(u) = \sup_{t\in[0,T]} \max_{x\in[-a,a]} \frac{|u^*(x,t) - \widehat{u}_n(x,t)|}{|u^*(x,t)|},$$

$$\mathrm{EOC}_n = \frac{\log\left(\frac{e_{n/2}(u)}{e_n(u)}\right)}{\log 2}, \quad \mathrm{EOC}_{\mathrm{mean}} = \frac{1}{M-2}\sum_{k=3}^{M} \mathrm{EOC}_{2^k}.$$

in suitable tables.

Example 5.1.

$$\begin{aligned} &u^*(x,t) = x^2 t, \\ &r = \frac{1}{2}, \quad \varphi(y-x) = \sin(y-x), \\ &u(\mathbf{x},0) = (0,\dots,0), \quad u(-a,t) = u(a,t) = a^2 t. \end{aligned} \tag{40}$$

Table 1 displays the results obtained for the problem (40) considered in Example 5.1 when the solution is $u^*(x,t) = x^2 t$. In this case, the kernel is oscillating and the two Dirichlet boundary conditions coincide.

The column of the empirical error values shows a fast convergence initially, then oscillations around the theoretical value of 4. The mean empirical error summarizes in this case the error behaviour.

Example 5.2.

$$\begin{aligned} &u^*(x,t) = x + t^2, \\ &r = \frac{1}{\pi}, \quad \varphi(y-x) = e^{-(y-x)}, \\ &u(\mathbf{x},0) = (x_0,\dots,x_n), \quad u(-a,t) = -a + t^2, \quad u(a,t) = a + t^2. \end{aligned} \tag{41}$$

In Example 5.2 the exact solution is $u^*(x,t) = x+t^2$. The kernel taken in consideration is $\varphi(y-x) = e^{-(y-x)}$; the boundary conditions are different, namely $u(\pm a,t) = \pm a + t^2$. The numerical results are reported in Table 2.

Table 3
Example 5.3, problem (42) — Empirical Order of Convergence.

n	$e_n(u)$	EOC_n
8	3.10e−03	
16	1.19e−03	1.38
32	5.85e−06	7.67
64	1.06e−06	2.46
128	9.44e−08	3.49
256	7.89e−09	3.58
512	1.19e−09	2.73
	$\mathrm{EOC}_{\mathrm{mean}}$	3.55

In this case the empirical error column values show initially a higher rate than expected, which is slowly decreasing to the theoretical value.

Example 5.3.

$$\begin{aligned} &u^*(x,t) = e^{x+\frac{t}{5}}, \\ &r = \frac{1}{3}, \quad \varphi(y-x) = \cos^2(y-x), \\ &u(\boldsymbol{x},0) = (e^{x_0},\dots,e^{x_n}), \quad u(-a,t) = e^{-a+\frac{t}{5}}, \quad u(a,t) = e^{a+\frac{t}{5}}. \end{aligned} \tag{42}$$

Example 5.3, whose results are shown in Table 3, examines the case in which the solution is of exponential type and the Dirichlet boundary conditions do not coincide.

Here the empirical error column values oscillate showing a slightly degraded performance with respect to the theoretical order expected.

Remark 5.4. Note that when $n = 512$, i.e. the grid in $[-2,2]$ consists of 513 equally spaced points, the exact solution $u^*(x,t)$ of the three examples is approximated with a precision of almost 10 significant digits. Moreover, the Mean Empirical Order of Convergence in all the cases is around 4 as expected by the convergence result, Theorem 4.1. Indeed, finite difference schemes of order 4 are used and the kernel is sufficiently smooth in all these cases.

5.2. Numerical simulations in population theory

Since we already tested the good performances of the method in the previous subsection, the following three examples provide simulations in the context of population theory, which lies at the root of the formulation (4).

The analytical solutions however are not known. Therefore our main goal is to study their behaviour for different choices of the parameters and operators, i.e. the population reproduction rate r and the nonlocal operator $\mathcal{K}(u,x,t)$ affecting how individuals reproduce due to resources found at a distance from their present location. We also vary the initial conditions $k(x)$ and the Dirichlet boundary conditions $b_{\pm}(t)$. Recall that in this context $u(x,t)$ and $\varphi(y-x)$ are non-negative functions because the $u(x,t)$ represents the size of a biological population.

Example 5.5.

$$\begin{aligned} &r = \frac{1}{2}, \quad \varphi(y-x) = e^{-(y-x)}, \\ &u(\boldsymbol{x},0) = \left(e^{\frac{x_0^3}{10}},\dots,e^{\frac{x_n^3}{10}} \right), \quad u(-a,t) = e^{\frac{-a^3}{10}} + t, \quad u(a,t) = e^{\frac{a^3}{10}} + t. \end{aligned} \tag{43}$$

In Example 5.5 the Dirichlet boundary conditions for the reference problem (43) are different, i.e. $b_-(t) = e^{\frac{-a^3}{10}} + t$ and $b_+(t) = e^{\frac{a^3}{10}} + t$. Fig. 1(a) shows how these conditions influence the population growth near the boundaries of the space domain. With the chosen kernel $\varphi(y-x) = e^{-(y-x)}$ and reproduction rate $r = \frac{1}{2}$ the population increases significantly in the interval $[0,2]$, while in the other half of it $[-2,0]$ the growth is slowed down by higher mortality. This behaviour can be observed also in Fig. 1(b), although the oscillating boundary conditions $b_{\pm}(t) = \sin(2t) + 2$ impose a periodic decrease of the population in time. Note that the scale used for the vertical axis of this plot differs from the other frames of Fig. 1, to better show the behaviour of the solution of the model. Fig. 1(c) considers the case in which the reproduction rate r is higher w.r.t. the reference problem which induces the peak in the interval $[1,2]$ and by the less drastic decrease of population in the opposite half of the space domain. Finally, Fig. 1(d) examines the opposite situation, where $r = \frac{1}{\pi}$. Here again, the peaks are guaranteed by the boundary conditions, but at the centre of the space domain, a sort of equilibrium between the number of births and deaths is achieved, lasting in time and leading there to a stagnation of the population size.

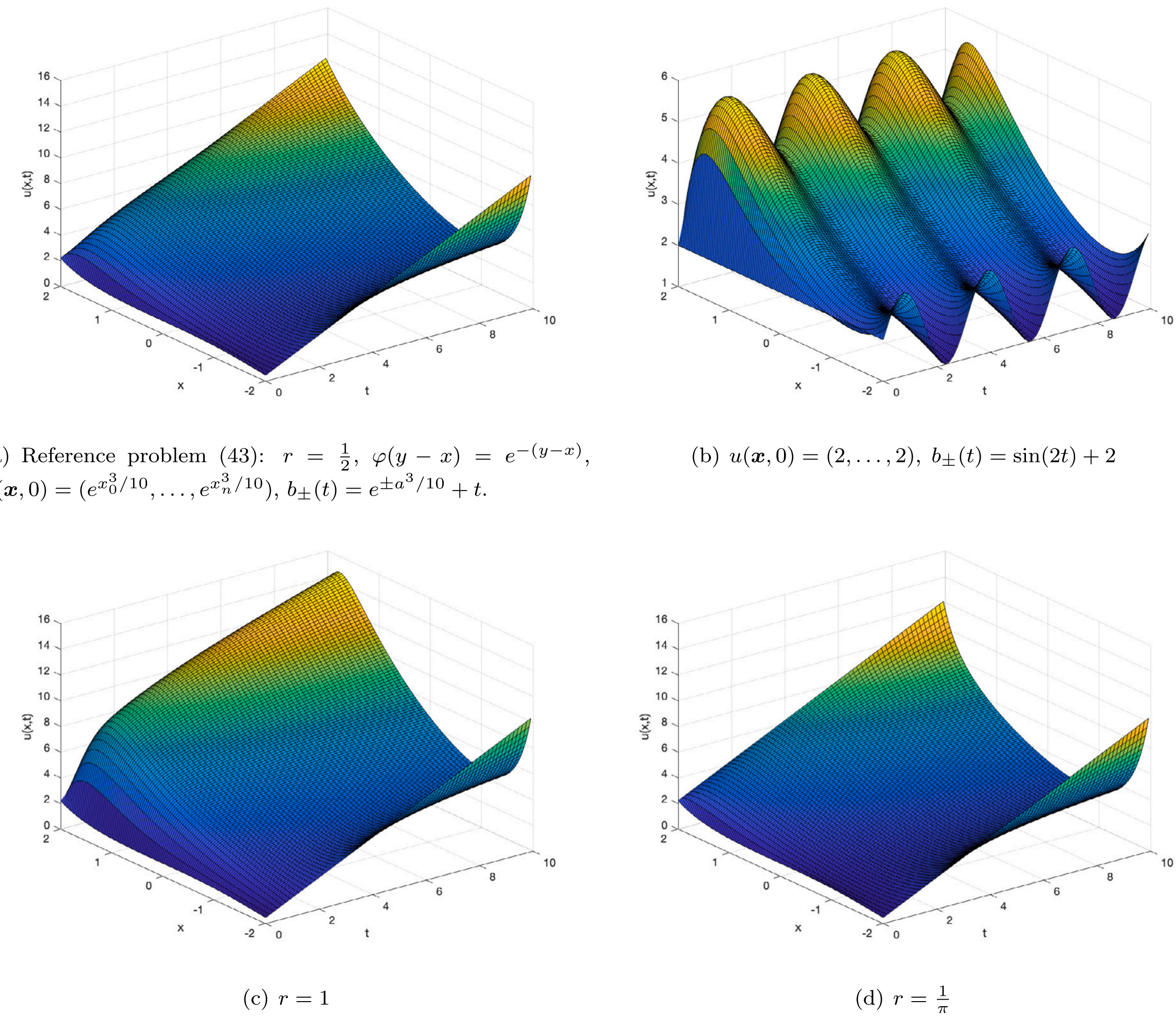

(a) Reference problem (43): $r = \frac{1}{2}$, $\varphi(y-x) = e^{-(y-x)}$, $u(\boldsymbol{x},0) = (e^{x_0^3/10}, \ldots, e^{x_n^3/10})$, $b_{\pm}(t) = e^{\pm a^3/10} + t$.

(b) $u(\boldsymbol{x},0) = (2,\ldots,2)$, $b_{\pm}(t) = \sin(2t) + 2$

(c) $r = 1$

(d) $r = \frac{1}{\pi}$

Fig. 1. Example 5.5.

Example 5.6.

$$
\begin{aligned}
&r = 1, \quad \varphi(y-x) = 2 + \sin(y-x), \\
&u(\boldsymbol{x},0) = (1,\ldots,1), \quad u(-a,t) = u(a,t) = \frac{t^2}{7} + 1.
\end{aligned}
\tag{44}
$$

Fig. 2 illustrates the results obtained for Example 5.6. The reference problem (44) is depicted in frame (a). It considers the case in which the reproduction rate is equal to 1 and the kernel is of oscillatory type. A general increase of the population size is observed for early times followed by a progressive downturn of the births, with an exception near the space domain endpoints, due to the effect of the boundary conditions $b_{\pm}(t) = \frac{t^2}{7} + 1$. Fig. 2(b) is in agreement with the behaviour observed in the reference problem with the only difference that in this case, there is a higher mortality near the endpoints of $[-2,2]$ because the new Dirichlet boundary conditions impose a slower exponential increase of the population there. In Fig. 2(c) the reproduction rate r is higher than the one of the reference problem; this leads to a higher increase in the population in time, with slightly higher mortality caused by the intraspecific competition in the half space domain $[0,2]$ due to a potential lack of resources for all the individuals. Finally, Fig. 2(d) depicts a generally slow growth of the population, because of the lower reproduction rate ($r = \frac{3}{4}$) w.r.t. the reference problem. Also in this case the peak at the endpoints of the space domain can be referred to the effect of the boundary conditions.

Example 5.7.

$$
r = \frac{5}{4}, \quad \varphi(y-x) = \cos^2(y-x),
\tag{45}
$$

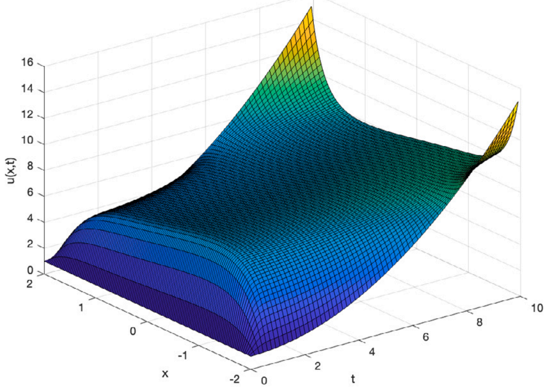

(a) Reference problem (44): $r = 1$, $\varphi(y - x) = 2 + \sin(y - x)$, $u(\boldsymbol{x}, 0) = (1, \ldots, 1)$, $b_{\pm}(t) = \frac{t^2}{7} + 1$.

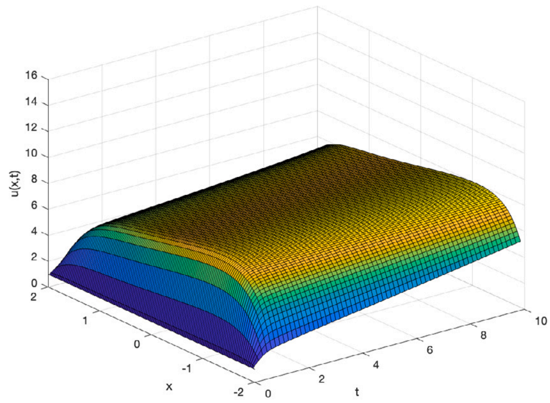

(b) $u(\boldsymbol{x}, 0) = (1, \ldots, 1)$, $b_{\pm}(t) = e^{\frac{\sqrt{t}}{2}}$

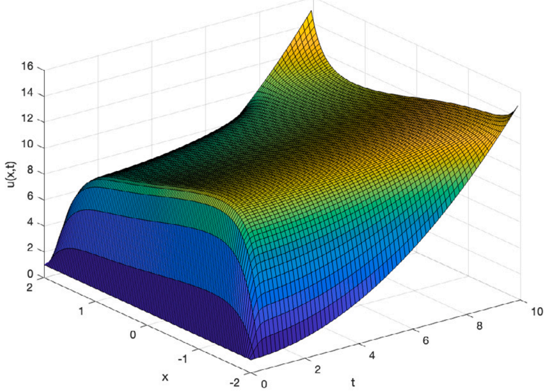

(c) $r = \frac{3}{2}$

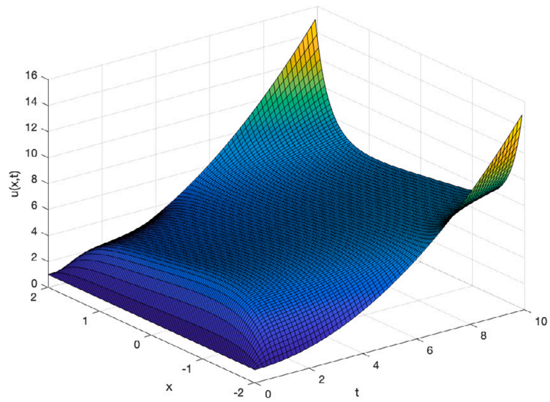

(d) $r = \frac{3}{4}$

Fig. 2. Example 5.6.

$$u(\boldsymbol{x}, 0) = (\log 3, \ldots, \log 3), \quad u(-a, t) = u(a, t) = \log(2t + 3).$$

In Example 5.7 the reproduction rate r is $\frac{5}{4}$, with identical Dirichlet boundary conditions of logarithmic type. The numerical solution $\hat{u}_n(x, t)$ for this reference problem (45) is displayed in Fig. 3(a). The population growth follows the logarithmic behaviour imposed by the boundary conditions, with slightly higher mortality due to the intraspecific competition around the centre of the spatial interval. In Fig. 3(b) the boundary conditions oscillate, namely $b_{\pm}(t) = \sin\left(\frac{t^2}{5}\right) + \frac{5}{2}$. We note a behaviour essentially similar to the one of the reference problem, but repeated in time following the oscillations of $b_{\pm}(t)$. Fig. 3(c) and Fig. 3(d) examine how the population is influenced by an increase, respectively a decrease, of the reproduction rate r. The plot in frame (c) shows a stronger growth of the population in time, having attenuated peaks in the subintervals $[-2, -1]$ and $[1, 2]$. At the centre of the space domain a higher mortality rate is observed, but significantly mitigated by the higher births overcoming the deaths. Finally, frame (d) depicts the opposite situation, where the births do not suffice to compensate for the intraspecific competition, leading to a stagnation of the population size, especially at the centre of the space domain. This tendency is reversed only approaching the endpoints of $[-2, 2]$, due to the effect of the Dirichlet boundary conditions.

Data availability

Data will be made available on request.

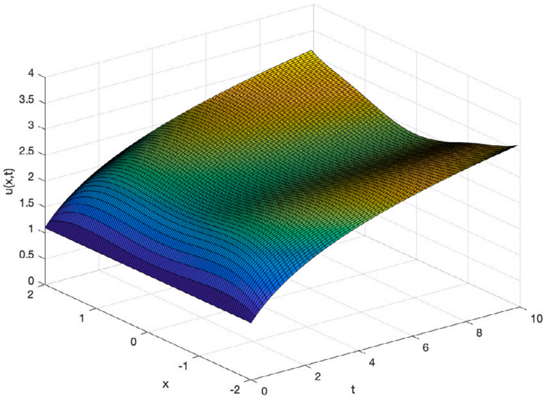

(a) Reference problem (45): $r = \frac{5}{4}$, $\varphi(y-x) = \cos^2(y-x)$, $u(\boldsymbol{x},0) = (\log 3, \dots, \log 3)$, $b_{\pm}(t) = \log(2t+3)$.

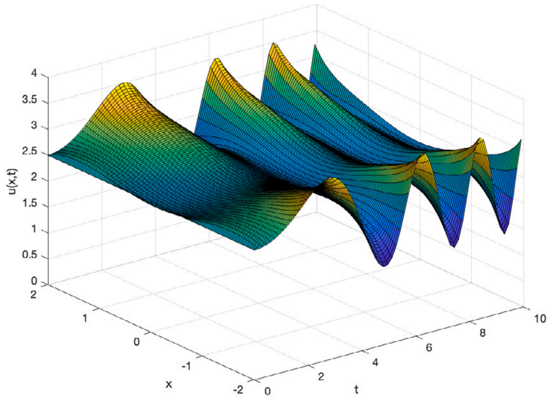

(b) $u(\boldsymbol{x},0) = \left(\frac{5}{2}, \dots, \frac{5}{2}\right)$, $b_{\pm}(t) = \sin\left(\frac{t^2}{5}\right) + \frac{5}{2}$

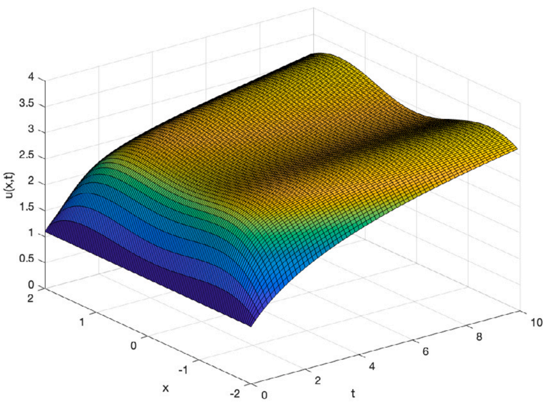

(c) $r = \frac{\pi}{2}$

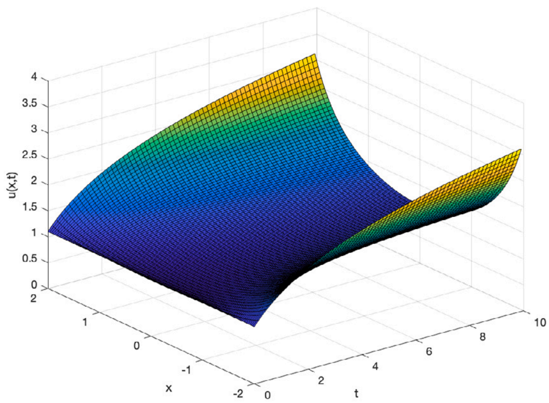

(d) $r = \frac{1}{3}$

Fig. 3. Example 5.7.

Acknowledgements

The authors thank the referees for their remarks, that contributed to the improvement of the presentation.

E.V. has been partially supported by the project "Metodi di approssimazione e modelli per le scienze della vita" (Approximation methods and models for the life sciences) of the Department of Mathematics "Giuseppe Peano" of the University of Turin. D.M. has been partially supported by GNCS-INdAM 2023 project "Approssimazione ed integrazione multivariata con applicazioni ad equazioni integrali"and by the Spoke 1 "FutureHPC & BigData"of ICSC - Centro Nazionale di Ricerca in High-Performance Computing, Big Data and Quantum Computing, funded by European Union - NextGenerationEU. D.O. has been partially supported by PRIN 2022 PNRR project no. P20229RMLB financed by the European Union - NextGeneration EU and by the Italian Ministry of University and Research (MUR). This research has been accomplished within RITA (Research ITalian network on Approximation) and the UMI Group TAA (Approximation Theory and Applications).

References

[1] D. Mezzanotte, D. Occorsio, E. Venturino, Analysis of a line method for reaction-diffusion models of nonlocal type, Appl. Numer. Math. (2024).
[2] T.R. Malthus, An essay on the principle of population, printed for J. Johnson in St. Paul's Churchyard, London, 1798.
[3] P.F. Verhulst, Notice sur la loi que la population suit dans son accroissement, in: Correspondance MathÉmatique Et Physique 10, Académie Royale de Bruxelles, Bruxelles, 1838, pp. 113–121.
[4] P.F. Verhulst, Recherches mathématiques sur la loi d'accroissement de la population, Mém. Acad. Roy. Bruxelles 18 (1845) 14–54.
[5] P.F. Verhulst, Recherches mathématiques sur la loi d'accroissement de la population, Mém. Acad. Roy. Bruxelles 20 (1847) 1–32.

[6] F.M.D. Gulland, The impact of infectious diseases on wild animal populations - a review, in: Ecology of Infectious Diseases in Natural Populations, Cambridge Univ. Press, 1995.
[7] S.P. Rushton, P.W.W. Lurz, J. Gurnell, P. Nettleton, C. Bruemmer, M.D.F. Shirley, A.W. Sainsbury, Disease threats posed by alien species: the role of a poxvirus in the decline of the native red squirrel in britain, Epidemiol Infect. 134 (2006) 521–533.
[8] D.M. Tompkins, A.R. White, M. Boots, Ecological replacement of native red squirrels by invasive greys driven by disease, Ecol. Lett. 6 (2003) 189–196.
[9] J.C. Reynolds, Details of the geographic replacement of the red squirrel (*Sciurus vulgaris*) by the grey squirrel (*Sciurus carolinensis*) in eastern England, J. Anim. Ecol. 54 (1985) 149–162.
[10] A.J.J. Chmaj, X. Ren, Pattern formation in the nonlocal bistable equation, Methods Appl. Anal. 8 (2001) 369–386.
[11] H. Malchow, S. Petrovskii, E. Venturino, Spatiotemporal patterns in Ecology and Epidemiology, Chapman & Hall/CRC, 2007.
[12] S. Genieys, V. Volpert, P. Auger, Pattern and waves for a model in population dynamics with nonlocal consumption of resources, Math. Model. Nat. Phenom. 1 (1) (2006) 63–80.
[13] V. La Morgia, E. Venturino, Understanding hybridization and competition processes between hare species: implications for conservation and management on the basis of a mathematical model, Ecol. Model. 364 (2017) 13–24.
[14] R.D. Holt, Predation, apparent competition and the structure of prey communities, Theor. Popul. Biol. 12 (1977) 197–229.
[15] E. Caudera, S. Viale, S. Bertolino, J. Cerri, E. Venturino, A mathematical model supporting a hyperpredation effect in the apparent competition between invasive eastern cottontail and native European hare, Bull. Math. Biol. 83 (2021) 51.
[16] X. Chen, Existence, uniqueness, and asymptotic stability of traveling waves in non-local evolution equations, Adv. Differential Equations 2 (1) (1997) 125–160.
[17] S.A. Gourley, Travelling front solutions of a nonlocal Fisher equation, J. Math. Biol. 41 (3) (2000) 272–284.
[18] A. Moussaoui, V. Volpert, Speed of wave propagation for a nonlocal reaction–diffusion equation, Appl. Anal. 99 (13) (2020) 2307–2321.
[19] S. Trofimchuk, V. Volpert, Traveling waves in delayed reaction-diffusion equations in biology, Math. Biosci. Eng. 17 (6) (2020) 6487–6514.
[20] P.W. Bates, A.J.J. Chmaj, An integrodifferential model for phase transitions: stationary solutions in higher space dimensions, J. Stat. Phys. 95 (1999) 1119–1139.
[21] V. Vougalter, V. Volpert, Solvability of some systems of integro-differential equations in population dynamics depending on the natality and mortality rates, Arnold Math. J. (2023).
[22] C.M. Elliott, S. Zheng, On the Cahn-Hilliard equation, Arch. Ration. Mech. Anal. 96 (1986) 339–357.
[23] P.W. Bates, J. Han, Neumann boundary problem for the nonlocal Cahn-Hilliard equation, J. Differential Equations 212 (2) (2005) 235–277.
[24] P.W. Bates, J. Han, The Dirichlet boundary problem for the nonlocal cahn-hilliard equation, J. Math. Anal. Appl. 311 (1) (2005) 289–312.
[25] P.W. Bates, On some nonlocal evolution equations arising in materials science, Nonlin. Dyn. Evolut. Equ. Fields Inst. Commun. 48 (2006) 13–52.
[26] P.W. Bates, J. Han, G. Zhao, On a nonlocal phase-field system, Nonlinear Anal. TMA 64 (10) (2006) 2251–2278.
[27] A. Baskaran, Z. Hu, J.S. Lowengrub, C. Wang, S.M. Wise, P. Zhou, Energy stable and efficient finite-difference nonlinear multigrid schemes for the modified phase field crystal, J. Comput. Phys. 250 (4) (2013) 270–292.
[28] P.W. Bates, S. Brown, J. Han, Numerical analysis for a nonlocal allen-cahn equation, Int. J. Numer. Anal. Model. 6 (1) (2009) 33–49.
[29] C. Cortazar, M. Elgueta, J.D. Rossi, Nonlocal diffusion problems that approximate the heat equation with Dirichlet boundary conditions, Israel J. Math. 170 (2009) 53–60.
[30] Z. Ditzian, W. Totik, Moduli of smoothness, SCMG Springer-Verlag, New York Berlin Heidelberg London Paris Tokyo, 1987.
[31] H.H. Gonska, X.l. Zhou, Approximation theorems for the iterated boolean sums of Bernstein operators, J. Comput. Appl. Math. 53 (1) (1994) 21–31.
[32] L. Fermo, D. Mezzanotte, D. Occorsio, A product integration rule on equispaced nodes for highly oscillating integrals, Appl. Math. Lett. 136 (2023) 108463.
[33] D. Occorsio, M.G. Russo, W. Themistoclakis, Some numerical applications of generalized Bernstein operators, Constr. Math. Anal. 4 (2) (2021) 186–214.
[34] D. Mezzanotte, D. Occorsio, M.G. Russo, E. Venturino, A discretization method for nonlocal diffusion type equations, Ann. Univ. Ferrara 68 (2) (2022) 505–520.
[35] D. Occorsio, M.G. Russo, Nyström methods for fredholm integral equations using equispaced points, Filomat 28 (1) (2014) 49–63.
[36] B. Fornberg, Generation of finite difference formulas on arbitrarily spaced grids, Math. Comp. 51 (184) (1988) 699–706.
[37] K.E. Atkinson, An Introduction to Numerical Analysis, Wiley, NY, 1978.
[38] K.E. Atkinson, Elementary Numerical Analysis, Wiley, NY, 1993.